
3-1-2007

Transcranial Doppler Estimation of Cerebral Blood Flow and Cerebrovascular Conductance During Modified Rebreathing

Jurgen A.H.R. Claassen
Radboud University Medical Center

Rong Zhang
UT Southwestern Medical Center

Qi Fu
UT Southwestern Medical Center

Sarah Witkowski
UT Southwestern Medical Center, switkowski@smith.edu

Benjamin D. Levine
UT Southwestern Medical Center

Follow this and additional works at: https://scholarworks.smith.edu/ess_facpubs



Part of the [Exercise Science Commons](#), and the [Sports Studies Commons](#)

Recommended Citation

Claassen, Jurgen A.H.R.; Zhang, Rong; Fu, Qi; Witkowski, Sarah; and Levine, Benjamin D., "Transcranial Doppler Estimation of Cerebral Blood Flow and Cerebrovascular Conductance During Modified Rebreathing" (2007). Exercise and Sport Studies: Faculty Publications, Smith College, Northampton, MA. https://scholarworks.smith.edu/ess_facpubs/29

This Article has been accepted for inclusion in Exercise and Sport Studies: Faculty Publications by an authorized administrator of Smith ScholarWorks. For more information, please contact scholarworks@smith.edu

Transcranial Doppler estimation of cerebral blood flow and cerebrovascular conductance during modified rebreathing

Jurgen A. H. R. Claassen,^{1,2} Rong Zhang,² Qi Fu,² Sarah Witkowski,² and Benjamin D. Levine²

¹Department of Geriatric Medicine, Radboud University Nijmegen Medical Center, The Netherlands; and

²Institute for Exercise and Environmental Medicine, Presbyterian Hospital of Dallas and The University of Texas Southwestern Medical Center at Dallas, Dallas, Texas

Submitted 16 August 2006; accepted in final form 12 November 2006

Claassen JA, Zhang R, Fu Q, Witkowski S, Levine BD. Transcranial Doppler estimation of cerebral blood flow and cerebrovascular conductance during modified rebreathing. *J Appl Physiol* 102: 870–877, 2007. First published November 16, 2006; doi:10.1152/jappphysiol.00906.2006.—Clinical transcranial Doppler assessment of cerebral vasomotor reactivity (CVMR) uses linear regression of cerebral blood flow velocity (CBFV) vs. end-tidal CO₂ (PETCO₂) under steady-state conditions. However, the cerebral blood flow (CBF)-PETCO₂ relationship is nonlinear, even for moderate changes in CO₂. Moreover, CBF is increased by increases in arterial blood pressure (ABP) during hypercapnia. We used a modified rebreathing protocol to estimate CVMR during transient breath-by-breath changes in CBFV and PETCO₂. Ten healthy subjects (6 men) performed 15 s of hyperventilation followed by 5 min of rebreathing, with supplemental O₂ to maintain arterial oxygen saturation constant. To minimize effects of changes in ABP on CVMR estimation, cerebrovascular conductance index (CVCi) was calculated. CBFV-PETCO₂ and CVCi-PETCO₂ relationships were quantified by both linear and nonlinear logistic regression. In three subjects, muscle sympathetic nerve activity was recorded. From hyperventilation to rebreathing, robust changes occurred in PETCO₂ (20–61 Torr), CBFV (–44 to +104% of baseline), CVCi (–39 to +64%), and ABP (–19 to +23%) (all $P < 0.01$). Muscle sympathetic nerve activity increased by 446% during hypercapnia. The linear regression slope of CVCi vs. PETCO₂ was less steep than that of CBFV (3 vs. 5%/Torr; $P = 0.01$). Logistic regression of CBF-PETCO₂ ($r^2 = 0.97$) and CVCi-PETCO₂ ($r^2 = 0.93$) was superior to linear regression ($r^2 = 0.91$, $r^2 = 0.85$; $P = 0.01$). CVMR was maximal (6–8%/Torr) for PETCO₂ of 40–50 Torr. In conclusion, CBFV and CVCi responses to transient changes in PETCO₂ can be described by a nonlinear logistic function, indicating that CVMR estimation varies within the range from hypocapnia to hypercapnia. Furthermore, quantification of the CVCi-PETCO₂ relationship may minimize the effects of changes in ABP on the estimation of CVMR. The method developed provides insight into CVMR under transient breath-by-breath changes in CO₂.

blood pressure; carbon dioxide

THE PROMINENT CEREBRAL BLOOD flow (CBF) responses to changes in arterial CO₂ are a unique characteristic of the cerebral vasculature (2, 27). These responses have been quantified to reflect cerebral vasomotor reactivity (CVMR) (44), even though the underlying mechanisms are still not completely understood (23). With the advent of transcranial Doppler (TCD) for measurement of CBF velocity (CBFV) with high temporal resolution, the Doppler-CO₂ test of CVMR has become a widely adopted method in research and clinical prac-

tice. Research exploring the physiological characteristics of CVMR has demonstrated that the relationship between arterial CO₂ and CBF is nonlinear and that this relationship is affected by CO₂-induced changes in arterial blood pressure (ABP) (11, 13, 14, 18, 31, 38, 39, 42, 44). In addition, the control mechanisms that govern the responses of CBF and ABP to CO₂ have dynamic properties (11, 31, 39). Despite these complexities associated with the CBF-CO₂ relationship, measurement of CVMR has been widely applied in clinical practice to evaluate cerebral vascular function, e.g., in patients with carotid artery stenosis or hypertension (5, 28, 44, 53). These clinical studies have quantified CVMR using linear regression of steady-state responses of CBF to changes in CO₂, without incorporation of the effects of ABP. The likely reason for this simplicity is that well-controlled experiments and complex modeling methods may not be practical for clinical use (31, 32). In this regard, development of a new method that is clinically applicable and may assess CVMR reliably under conditions of breath-by-breath changes in end-tidal CO₂ (PETCO₂) is warranted.

We used a modified rebreathing protocol, consisting of a period of voluntary hyperventilation, followed by rebreathing, to obtain a wide range of changes in PETCO₂ to assess CVMR under breath-by-breath conditions (10). We hypothesized that the CBF-PETCO₂ relationship is nonlinear during transient changes in PETCO₂. In addition, we speculated that measurement of cerebrovascular conductance index (CVCi) during this process may reveal direct effects of changes in ABP on CBF, leading to a more precise estimation of CVMR based on the CVCi-PETCO₂ relationship. Finally, to explore the underlying mechanisms of increases in ABP during hypercapnia, we recorded muscle sympathetic nerve activity (MSNA) in three subjects in this study.

METHODS

Ten healthy subjects (4 women) with a mean age of 37 yr (SD 8), height 177 cm (SD 10), and weight 84 kg (SD 18) voluntarily participated in the study. Participants were nonsmokers, were not on any medication, and were normotensive. Participants were free of known cardiovascular, cerebrovascular, or respiratory disease. Each subject was informed of the experimental procedures and signed a consent form, approved by the Institutional Review Boards of the University of Texas Southwestern Medical Center and Presbyterian Hospital of Dallas.

Protocol. Each participant visited the laboratory twice, 3–4 wk apart (in three participants, the time interval was 3–4 mo). All experiments took place in a quiet laboratory with a room temperature

Address for reprint requests and other correspondence: R. Zhang, Institute for Exercise and Environmental Medicine, Presbyterian Hospital of Dallas, 7232 Greenville Ave., Dallas, TX 75231 (e-mail: RongZhang@texashealth.org).

The costs of publication of this article were defrayed in part by the payment of page charges. The article must therefore be hereby marked “advertisement” in accordance with 18 U.S.C. Section 1734 solely to indicate this fact.

of 22°C. The subjects refrained from heavy exercise and caffeinated or alcoholic beverages at least 12 h before the tests. The study was conducted with the subjects in the supine position. Therefore, assessment of CVMR would be comparable with those obtained with other imaging technology (32). Participants wore a nose clip and breathed through a mouthpiece with a Y-valve, with one end connected to a 5-liter rubber bag and the other end open to room air. This system was held in place by an adjustable cable, rendering it practically weightless to avoid any discomfort for the subject. After at least 20 min of stabilization, 2 min of baseline data during spontaneous breathing were recorded on room air. A modified Read rebreathing protocol was used (10, 33, 51). The procedure contains a period of voluntary hyperventilation preceding rebreathing to obtain a wider range of CO₂ changes. Specifically, a short period of 15 s of hyperventilation with a duty cycle of 1 s and maximal voluntary deep breaths were used. This short period of hyperventilation reduced PETCO₂ to ~20 Torr but did not cause respiratory muscle fatigue or central hypoxia possibly associated with a prolonged hyperventilation as employed in the other rebreathing methods (33, 51). At the end of a deep inspiration, the respiratory valve was switched to the empty bag and then the bag was filled with the subjects' own breathing gas during expiration (with a PETCO₂ of ~20 Torr, comparable to a gas mixture with 2.6% CO₂). Rebreathing was continued for 5 min, before returning to room air for recovery (4 min). During rebreathing, a small amount of oxygen was bled into the rebreathing bag at the subject's basal metabolic rate (estimated using the Harris-Benedict formula) to maintain arterial oxygen saturation (SaO₂) constant (19).

Instrumentation and data acquisition. The middle cerebral artery (MCA) was insonated with a 2-MHz pulsed Doppler ultrasound system (Multi-Dope X2; DWL). The probe was securely attached to the cranium by a mold that was cast individually to fit the facial bone structure (16). In this way, the exact position and angle of the probe were preserved during the repeat tests.

Throughout the test, ABP was monitored noninvasively using a Finapres (Ohmeda 2300) and was corroborated by concurrent electrophygmomanometry (SunTech Medical) with measurements at intervals of 1 min. PETCO₂ was recorded using a capnograph (POET TE; Criticare Systems), SaO₂ was measured using a pulse oximeter (Biox 3700; Ohmeda), and heart rate (HR) was monitored with a three-lead ECG connected to a cardiachometer (Quinton Instruments).

MSNA was recorded in three participants. MSNA signals were obtained by the microneurographic technique (50). Sympathetic bursts were identified by a computer program and then were confirmed by an experienced microneurographer. The number of bursts per minute (burst frequency) and the sum of the integrated burst area per minute (total activity) were used as quantitative indexes. Specifically, total activity was normalized to the baseline value (set at 100%) to reflect changes in sympathetic activity during CO₂ stimuli.

Data analysis. Off-line data analysis was performed with commercially available software (Acknowledge; BIOPAC Systems). For hyperventilation, the time delay between the onset of hyperventilation and the onset of changes in CBFV and ABP was measured. Similarly, at the end of rebreathing, the time delays for recovery between PETCO₂, CBFV, and ABP were measured. Values for CBFV, ABP, and PETCO₂ at the last minute of recovery were compared with their pretest baseline. Breathing cycles were identified from the respiratory CO₂ signal. For each cycle, the corresponding value for PETCO₂ and mean values for CBFV, ABP, and HR were measured. Averaging the number of cardiac cycles (usually 6) has been applied previously in an attempt to reduce respiratory hemodynamic variability (17). We preferred to identify each respiratory cycle (22) to derive the breath-to-breath CBFV-PETCO₂ relationship. During the short breathing cycles in hyperventilation, an average of data from two cycles was used. Because CBFV is affected directly by changes in ABP (11, 13, 27, 38), CVCi was calculated by dividing mean CBFV by mean ABP within each breath cycle to reveal intrinsic vascular responses to

changes in CO₂. Furthermore, percent changes from baseline CBFV and CVCi values were calculated for data analysis. Data ranging from the nadir of PETCO₂ during hyperventilation to the end of rebreathing were utilized for curve fitting to quantify the CBFV-PETCO₂ and CVCi-PETCO₂ relationship.

A four-parameter logistic function was used for curve fitting (26):

$$f(x) = y_0 - \frac{a}{1 + e^{[b \times (x - x_0)]}} \quad (1)$$

where $f(x)$ represents percent changes in CBFV or CVCi (x representing PETCO₂). The model parameter a represents the range of change in CBFV or CVCi, y_0 is the maximum value of CBFV or CVCi during hypercapnia, x_0 is the level of PETCO₂ where the first-order derivative of the logistic function (the slope of the curve) is maximal, and b is related to the overall curvilinear properties of the sigmoidal curve (Fig. 1). Nonlinear curve fitting was performed with a Marquardt-Levenberg algorithm for model parameter identification (SigmaPlot 8.02; SPSS). The selection of this model was based on the feature of curvilinear distribution of breath-by-breath changes in CBFV or CVCi vs. PETCO₂ (Fig. 2) and the fact that model parameters of the selected logistic function have clear physiological implications, as shown in Fig. 1 (26).

The first-order derivative of the logistic function was calculated with the following equation:

$$f'(x) = \frac{a \times b \times e^{[b \times (x - x_0)]}}{\{1 + e^{[b \times (x - x_0)]}\}^2} \quad (2)$$

This derivative function yields the specific CO₂ sensitivity (or CVMR) for each PETCO₂. At $x = x_0$, CVMR becomes maximal (CVMRmax), and Eq. 2 becomes $(a \times b)/4$. Of note, CVMRmax derived from the CBFV-PETCO₂ relationship was denoted as CBFV-CVMRmax and CVMRmax derived from the CVCi-PETCO₂ relationship was denoted as CVCi-CVMRmax.

For comparison, linear regressions of changes in CBFV and CVCi vs. PETCO₂ were conducted for the entire range of changes in PETCO₂, from the nadir of hyperventilation to the end of rebreathing. The slopes of these linear regressions were defined as CBFV-CVMR0 and CVCi-CVMR0, respectively. In addition, to complement the assessment of CVMRmax with the derivative method, CVMR was estimated by the linear regressions in the steep part of the sigmoidal curves, and these results were defined as CBFV-CVMR1 and CVCi-CVMR1, respectively.

Statistics. The results of curve fitting were examined by the correlation coefficients (r^2) and by model residual analysis of individual data (SigmaPlot 8.02; SPSS). Thus individual data for r^2 as well as mean sum of squares were available for both linear and

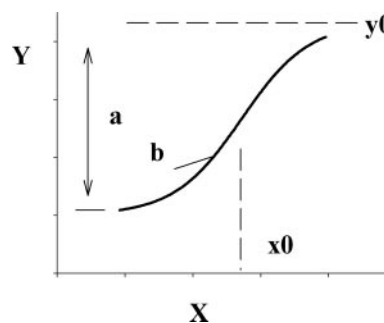
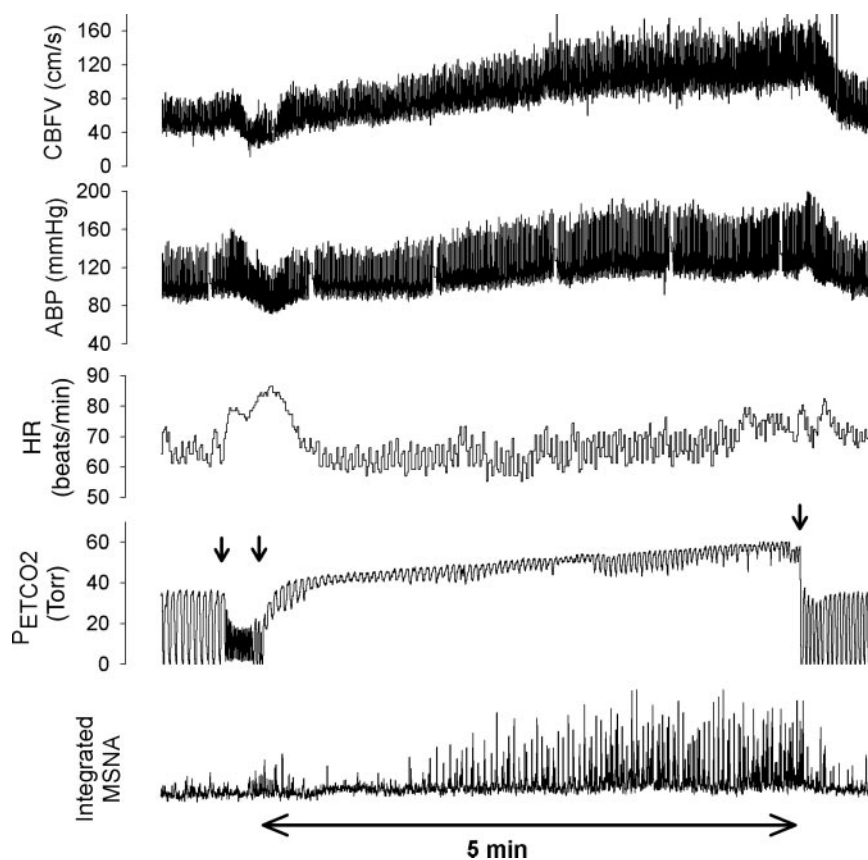


Fig. 1. Schematic representation of a logistic function with 4 parameters to be identified. a , Total range of changes in cerebrovascular conductance index (CVCi) or cerebral blood flow velocity (CBFV); y_0 , maximum value; x_0 , level of end-tidal CO₂ (PETCO₂) that exhibits highest CO₂ sensitivity; b , curvilinear properties of the sigmoidal curve.

Fig. 2. A typical recording of baseline, hyperventilation, rebreathing, and recovery in 1 subject. ABP, arterial blood pressure; HR, heart rate; MSNA, muscle sympathetic nerve activity. Note the significant increases in ABP and MSNA, concurrent with the increase in CBFV during rebreathing. Arrows indicate start and end of hyperventilation and rebreathing periods.



logistic curve fits, allowing comparisons of both methods on using paired *t*-tests (SigmaStat 3.11; Systat Software). Comparisons of cerebral hemodynamics at baseline, during hyperventilation, and during rebreathing were made with one-way repeated-measures ANOVA. Comparisons between the estimates of CVMR by different methods were made with paired *t*-tests. Test-retest reproducibilities for curve-fitting parameters and for CVMR estimation were examined by the analysis of typical error (the SD of the differences between the two tests divided by square root of 2), which was expressed as a coefficient of variation (21). Data are presented as means and SD, and a $P < 0.05$ was considered to be statistically significant.

RESULTS

Changes in cerebral and systemic hemodynamics. All 10 participants completed the experimental protocol, so that 20 data sets were collected. Data from one test could not be used because of poor signal quality; hence, reproducibility results were available only for nine subjects. Representative changes in CBFV, ABP, PET_{CO_2} , HR, and MSNA are shown in Fig. 2. Individual values for Sa_{O_2} varied within the range of 96–100% during baseline breathing of room air and remained unchanged during rebreathing, owing to the supplementation of oxygen. There was a delayed response of CBFV (mean: 7 s, range 6–10) and ABP (mean: 14 s, range 12–16) to changes in PET_{CO_2} during hyperventilation. Correction for the time delay did not significantly alter the result of data analysis. Because the physiological validity of applying a time correction for CVMR estimation was uncertain, analysis of the raw (uncorrected) data is presented. After the rapid return of PET_{CO_2} to the pretest baseline level

at the onset of recovery, a considerable time delay was observed for the ensuing recovery of CBFV (mean: 21 s, range 14–35) and of ABP (mean: 22 s, range 12–30). However, this delay did not influence the data analysis because the recovery period was not included in the models used to assess CVMR in this study. Whereas ABP gradually returned to the pretest baseline after rebreathing, CBFV displayed an undershoot and then gradually returned to a sustained level, which was below the pretest baseline level (mean: 81% of baseline, range 65–90), even at the end of the 4 min of recovery.

On average, PET_{CO_2} was reduced by 22 Torr during hyperventilation and increased by 20 Torr during rebreathing from the pretest baseline ($P < 0.001$). These changes in PET_{CO_2} resulted in a respective reduction of CBFV by 46% and an increase by 104% relative to the baseline ($P < 0.001$). CVCi fell by 39% during hyperventilation and increased by 64% during rebreathing ($P < 0.001$). Of note, ABP was reduced by 19% during hyperventilation and augmented by 23% during rebreathing ($P < 0.01$). During rebreathing, increases in ABP appeared to be proportional to increases in PET_{CO_2} but leveled off at high levels of PET_{CO_2} (Fig. 2). HR increased by 29% during hyperventilation and by 14% during rebreathing ($P < 0.01$) (Fig. 2, Table 1).

In the three subjects that underwent recording of MSNA, averaged burst frequency increased from 24 at baseline to 30 bursts/min during hyperventilation, and total nerve activity increased by 166% ($P = 0.01$). MSNA returned rapidly to baseline after cessation of hyperventilation and subsequently

Table 1. Changes in cerebral and systemic hemodynamics during the test

Subject	Baseline				Hyperventilation				Rebreathing			
	PETCO ₂	CBFV	MABP	HR	PETCO ₂	CBFV	MABP	HR	PETCO ₂	CBFV	MABP	HR
1	46	60	89	59	23	31	65	76	67	101	101	64
2	42	82	77	72	22	42	57	87	61	142	92	77
3	41	89	90	62	24	45	63	70	58	155	142	80
4	42	45	89	56	16	23	73	68	62	98	101	59
5	43	71	86	45	17	36	65	79	61	151	103	57
6	40	56	96	70	13	29	75	94	61	127	108	78
7	37	60	103	59	20	31	95	73	55	122	123	70
8	41	41	94	69	21	21	77	81	65	104	108	72
9	37	55	103	65	23	38	86	85	61	128	139	75
10	42	62	99	76	22	32	89	97	62	128	119	86
Mean	41	62	93	63	20*	33*	75*	81*	61*	126*	114*	72*
SD	3	15	8	9	4	8	12	10	3	20	17	9

Values are means from all available tests in $n = 10$ subjects. PETCO₂, end-tidal CO₂ (Torr); CBFV, cerebral blood flow velocity (cm/s); MABP, mean arterial blood pressure (mmHg); HR, heart rate (beats/min). Baseline, average of 2-min recordings before hyperventilation; hyperventilation, lowest values after 15 s of hyperventilation; rebreathing, average of the last minute of data. * $P < 0.01$ for comparison of hyperventilation and rebreathing with baseline.

increased to 41 bursts/min and 446% for total nerve activity during the last minute of rebreathing ($P = 0.01$; Fig. 2). Changes in MSNA were similar in all three subjects.

Curve-fitting and model parameters. Figure 3 depicts the representative results of sigmoidal curve fitting of the CBFV/CVCi-PETCO₂ relationship in one subject. The specific CVMR derived from the first-order derivative of the logistic function is also plotted.

The group-averaged data of changes in CBFV and CVCi as well as logistic regression of pooled data for all subjects are shown in Fig. 4. Because there were no significant differences between results from the first and second tests, all data were used in the pooled data analysis. Logistic regression of individual data demonstrated an excellent curve-fitting result (mean $r^2 = 0.95$, SD 0.04; average of mean sum of squares = 37, SD 19), superior to the use of linear regression (mean $r^2 = 0.88$, SD 0.06; average of mean sum of squares = 85, SD 51; $P < 0.01$) for both the CBFV-PETCO₂ and the CVCi-PETCO₂ relationships. Specifically, logistic regression was performed well in all 18 tests for changes in CBFV ($r^2 = 0.97$, SD 0.02) and in 16 of 18

tests for CVCi ($r^2 = 0.93$, SD 0.06). In those two cases of CVCi for which logistic regressions could not be performed reliably, linear regressions yielded an r^2 of 0.71 and 0.76 for CBFV and CVCi, respectively.

Table 2 shows the group-averaged model parameters and the calculated CVMR indexes derived, respectively, from the logistic and linear regressions. Over the entire range of changes in PETCO₂, the linear regression slope of changes in CVCi (CVCi - CVMR0) was significantly smaller than that of CBFV (CBFV - CVMR0). The steep ranges of the sigmoidal curves were found to lie between 40 and 50 Torr PETCO₂ for most subjects (Figs. 3 and 4). As expected, in the steep ranges of the sigmoidal curves, linear regression slopes of changes in CBFV (CBFV - CVMR1) and CVCi (CVCi - CVMR1) were similar to those obtained from the first-order derivatives of the identified logistic function (CBFV - CVMRmax and CVCi - CVMRmax, respectively). Of note, both CVMRmax and CVMR1 were higher than the estimates of CVMR from the linear regressions over the entire range of changes in PETCO₂ (CVMR0). Finally, for test-retest reproducibility, coefficients of varia-

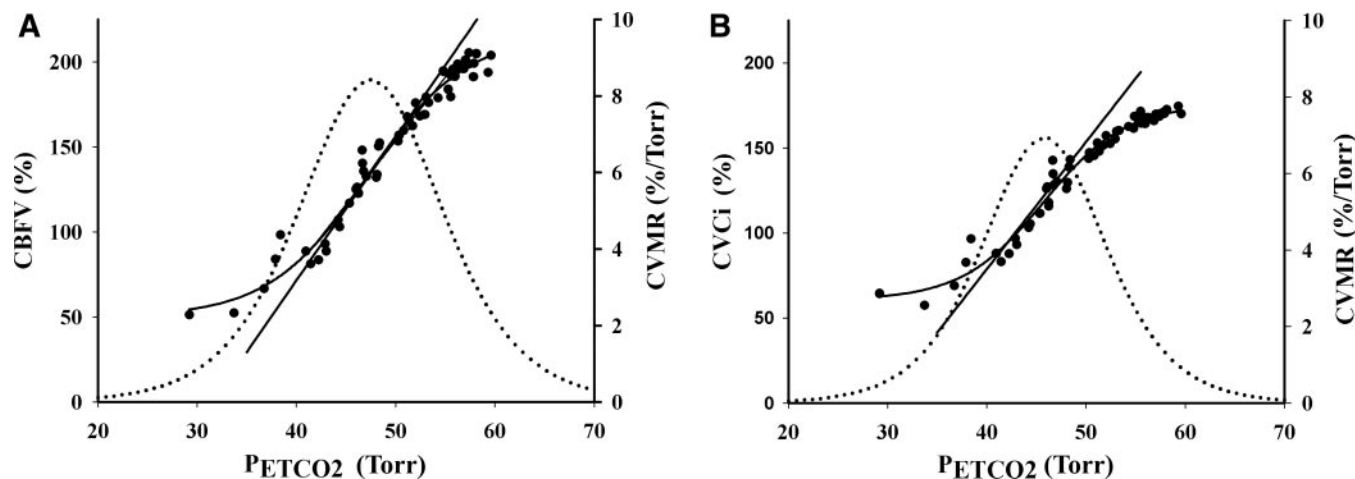
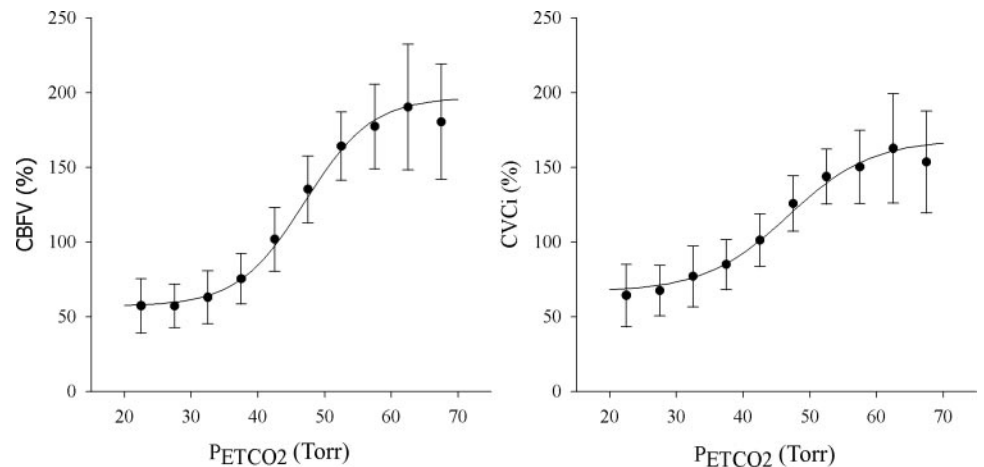


Fig. 3. Typical data of logistic regression of %changes in CBFV and CVCi to changes in end-tidal CO₂ (PETCO₂) in 1 subject. Sigmoidal curve represents the result of logistic regression; the dotted bell-shaped curve is the first-order derivative of the identified logistic function. Linear regression was performed in the steep portion of the sigmoidal curve to estimate cerebral vasomotor reactivity (CVMR), using CBFV and CVCi as the dependent variables, respectively.

Fig. 4. Group ($n = 10$) averaged results for logistic regression of percent changes in CBFV and CVCi to changes in P_{ETCO_2} . Sigmoidal curve represents the result of logistic regression of pooled group data from all subjects (parameters for CBFV: $a = 140\%$, $y_0 = 198\%$, $x_0 = 47$ Torr, $b = 0.20$ Torr $^{-1}$; parameters for CVCi: $a = 102\%$, $y_0 = 169\%$, $x_0 = 47$ Torr, $b = 0.16$ Torr $^{-1}$; note that these values are similar to the parameters obtained by averaging the individual curve fitting results as listed in Table 2). ● and error bars, Group averages and SDs, respectively, for CBFV (%) and CVCi (%) within 5-Torr ranges of P_{ETCO_2} (e.g., 20–25, 25–30, etc.).



tion for curve-fitting parameters and for estimates of CVMR are presented in Table 2.

DISCUSSION

We have developed a clinically applicable method to assess CVMR that addresses the nonlinear relationship and interactions between transient changes in CO_2 , CBFV, and ABP. Based on a modified rebreathing method, we have observed a wide range of breath-by-breath changes in P_{ETCO_2} (~20–61 Torr) and corresponding changes in CBFV, CVCi, and ABP.

The main findings of this study are twofold. First, consistent with our hypothesis, transient, breath-by-breath responses of both CBFV and CVCi to changes in P_{ETCO_2} demonstrate nonlinear properties that can be quantified by a logistic function. Second, the magnitude of increases in CBFV during hypercapnic rebreathing exceeded CVCi (104% vs. 64%) because of the presence of significant increases in ABP by 23%. Consistently, during hypocapnic hyperventilation, the reduction in CBFV (46%) surpassed CVCi (39%), whereas ABP fell by 19%. These observations suggest that changes in ABP during CO_2 stimuli have direct effects on CBF.

Table 2. Estimation of logistic function parameters and CVMR

	CBFV- P_{ETCO_2}	CV, %	CVCi- P_{ETCO_2}	CV, %
a , %	149 ± 34	17	99 ± 29*	26
y_0 , %	202 ± 35	10	166 ± 30*	11
x_0 , Torr	47 ± 2	6	46 ± 2	4
b , Torr $^{-1}$	0.22 ± 0.06	36	0.28 ± 0.09	58
CVMRmax,				
%Torr	8 ± 2†	23	6 ± 2†	31
CVMR0,				
%Torr	5 ± 1	18	3 ± 1*	18
CVMR1,				
%Torr	7 ± 1†	9	6 ± 1*†	26

Values are means ± SD from 10 subjects. CV, coefficient of variation; CBFV, cerebral blood flow velocity; a , y_0 , x_0 , and b , identified logistic function parameters (Fig. 1); CVMRmax, maximal cerebral vasomotor reactivity (CVMR), peak value of the first-order derivative of the identified logistic function; CVMR0: linear regression slope of percent changes in CBFV over the entire range of changes in P_{ETCO_2} ; CVMR1, linear regression slope of CBFV vs. P_{ETCO_2} in the steep portion of the sigmoidal curve. * $P < 0.01$ for difference in parameters between CBFV- P_{ETCO_2} and CVCi- P_{ETCO_2} . † $P < 0.01$ for CVMR0 vs. CVMRmax and CVMR1.

Study limitations. The reproducibility of model parameters and estimates of CVMR are comparable with other Doppler- CO_2 tests (44, 45, 48). Nonetheless, the coefficient of variation of the model parameter b was relatively large compared with the other parameters (Table 2). Parameter b reflects the overall curvilinear properties of the sigmoidal curve. Therefore, estimation of parameter b may have been affected by the lack of precise control of levels of P_{ETCO_2} reached during voluntary hyperventilation between the tests. The technique of dynamic end-tidal forcing may provide much better control of P_{ETCO_2} to improve the reproducibility of model parameter's estimation (40).

An additional limitation, inherent to the use of TCD, is that CBFV was measured to reflect changes in CBF. The TCD method has been well validated against other modalities used to measure CBF (4, 9, 30). However, changes in CBFV reflect changes in CBF only if the diameter of the insonated MCA remains constant. Direct and indirect measurements of the MCA diameters and comparisons of changes in CBFV with changes in CBF measured by different modalities during either hypo- or hypercapnia suggest the validity of using TCD (15, 46). We cannot exclude the possibility that a vasodilatation in the MCA may occur at high levels of CO_2 (49). If this were the case, the magnitude of maximal changes in CBF may have been underestimated by the measurement of CBFV during hypercapnia. However, the maximum changes in CBFV at a P_{ETCO_2} level of 60 Torr (~100% above baseline) are consistent with results of direct measurements of CBF in other studies with a similar level of changes in CO_2 (14, 27).

Magnitude of changes in CBFV and ABP. We found marked changes in CBFV with a range of nearly 150% from hyperventilation to rebreathing, with rebreathing accounting for an estimated doubling of baseline CBF. This range of changes in CBF is comparable with those found in other studies using TCD or other techniques to measure CBF (14, 24, 27, 35, 40, 51). Prominent CBF responses to arterial CO_2 are well established (23, 27, 42, 44). These changes in CBF have been attributed mainly to cerebral vasodilatation during hypercapnia and vasoconstriction during hypocapnia (3, 52).

However, changes in arterial CO_2 elicit complicated autonomic reflexes and exert vascular effects not only in the cerebral but also in the systemic circulation (29, 43). ABP increases substantially even during moderate increases in arte-

rial CO₂, due largely to sympathetic activation (6, 11, 38, 47), which clearly occurred in our study as well. This chemoreflex-mediated sympathetic activation may have confounding and opposing effects for the cerebral circulation, especially in the setting of CO₂-induced cerebral vasodilatation. For example, systemic hypertension may increase CBF prominently when normal autoregulatory mechanisms are impaired by CO₂ (13, 18, 37). Conversely, sympathetic activation in the brain may restrain CO₂-induced vasodilatation (7, 12, 52, 55), although it is less certain whether such effects occur consistently in humans (25). Both of these opposing effects will influence the measurement of CVMR during rebreathing.

In the present study, we found that estimates of CVMR based on CBFV (during either hyper- or hypocapnia) exceeded those based on CVCi. For example, model parameters a and y_0 (which reflect the range and maximal changes in CBFV and CVCi, respectively) derived from the CBFV-PETCO₂ relationship were significantly higher than those obtained from the CVCi-PETCO₂ relationship. Likewise, linear regressions resulted in higher values for CVMR when derived from CBFV instead of CVCi.

According to Ohm's law, the much higher increases in CBFV (104%) during hypercapnia relative to the increases in CVCi (64%) could be attributed to the 23% increase in ABP. Consequently, increases in ABP led to an overestimation of CVMR based on the linear regression of changes in CBFV vs. PETCO₂ (CBFV - CVMR0) (Table 2) (13). Together, these findings suggest that the net CBF responses to acute hypercapnia in humans are dominated by an overwhelming vasodilatory effect of CO₂, which impairs cerebral autoregulation and thereby enhances the effects of ABP on CBFV.

Estimation of CVCi. This study applies changes in cerebrovascular conductance to assess CVMR during transient changes in PETCO₂. The use of CVCi, in contrast to changes in CBFV, may better reflect the physiological process of cerebral vasodilatation during hypercapnia and cerebral vasoconstriction during hypocapnia. When an index of cerebrovascular resistance (the inverse of conductance) is used rather than CBFV to assess CVMR, the outcome was less influenced by changes in ABP (13). However, the use of resistance, rather than its inverse conductance, to assess CVMR may lead to difficulties in data interpretation, especially under conditions with increased CBF (34). Because of their reciprocal relationship, in a condition where resistance is low and blood flow is high, a large increase in conductance (vasodilatation) leads to only a small (further) decrease in resistance. Therefore, if vasomotor responses are estimated from changes in resistance, such a small decrease in resistance could be falsely interpreted to represent a small increase in vasodilatation. Because CVMR testing generates high blood flow, conductance rather than resistance was used in this study.

Alternatively, studies have analyzed the ABP-CBFV relationship within each cardiac cycle and used linear extrapolations to calculate the zero-flow pressure (also known as critical closing pressure) or resistance-area product indexes (1, 22, 36). Hypocapnia increases and hypercapnia reduces zero-flow pressure; therefore, changes in these indexes may serve as alternative measures to assess cerebrovascular responses to CO₂ (17, 22). Whereas the clinical relevance of assessment of CVMR has been demonstrated in follow-up studies in patients at risk

for cerebrovascular events (28, 53), similar findings have not been reported for zero-flow pressure or resistance-area product parameters.

Temporal characteristics of changes in CBFV and ABP. The CBF response to transient changes in CO₂ has a time delay of ~5–7 s (31, 41). It is therefore of interest to consider whether this factor could affect the estimation of CVMR using the proposed modeling. Identification of the time delay between transient changes in CBF and PETCO₂, as performed in these studies, requires complex and stringent control of respiration and CO₂ levels. However, in the present study, we are able to approximate the time delay between changes in PETCO₂, CBFV, and ABP based on the individual data from each subject. The average time delay of the reduction in CBFV in response to the reduction in PETCO₂ during hyperventilation was ~7 s, consistent with the reported time delay after a negative step change in PETCO₂ (6.8 s) (41) and with a time delay of ~5 s found when spontaneous CO₂ oscillations were analyzed (39). This time delay is possibly explained by CO₂ transportation time (54). The identification of a similar time delay during hypercapnic rebreathing is less evident because, as can be seen in Fig. 2, rebreathing caused a ramplike increase in PETCO₂. Despite the time delay between transient changes in CBFV and CO₂, it had little effect on the estimation of CVMR. With a total duration of hyperventilation of 15 s, a (short) plateau phase with minimum and stable CO₂ and CBFV values was reached in all individuals. Values at the end of hyperventilation (i.e., in this plateau phase) were used as a starting point for calculation of CVMR. Therefore, "correction" for the time delay did not affect the modeling and data outcome. Similarly, the observed reduction in ABP during hyperventilation also showed a time delay, lagging behind the changes in CBFV by an additional 7 s. This delayed response in ABP may partly explain why there was a smaller difference between changes in CVCi and CBFV during hyperventilation when compared with hypercapnic rebreathing.

During rebreathing, CBFV increased steadily, associated with a continuous increase in PETCO₂, and then appeared to level off at high levels of PETCO₂. Two mechanisms may have contributed to the saturation of CBFV. First, cerebral vasodilatation may have reached its maximal levels at or greater than a PETCO₂ of 60 Torr (42, 44). Second, substantial sympathetic activation may constrain the magnitude of the CBFV responses (7, 25, 52).

With the onset of recovery, PETCO₂ returned rapidly to the pretest baseline level within ~1–2 breaths of room air (<10 s). However, there was a substantial time delay of ~20 s for CBFV to reach a new sustained level, which was lower than the pretest baseline value. Of note, ABP returned to the pretest baseline level without a similar undershoot. These data suggest a sustained cerebral vasoconstriction during recovery from prolonged acute hypercapnia. In addition, these data confirm that adaptive processes modify the response in both ABP and CBF to CO₂, leading to limitations in the use of steady-state data to estimate CVMR (14, 41). However, the time delay in the recovery of CBFV appears to be much longer than that reported with a step change in CO₂ (6 s) (40). These discrepancies might be related to the differences in the duration as well as the intensities of CO₂ stimuli used.

Assessment of CVMR. A sigmoidal distribution of data was present in most subjects when breath-by-breath changes in CBFV were plotted against P_{ETCO_2} . Furthermore, similar distributions were observed for changes in CVCi, indicating the presence of threshold and saturation properties of cerebrovascular changes in response to transient changes in P_{ETCO_2} , providing further evidence for the nonlinear properties of CBF responses to changes in CO_2 (40–42, 44, 54). However, the specific physiological mechanisms underlying the nonlinear CBF- CO_2 relationship cannot be determined in the present study.

Data with a sigmoidal distribution could be fitted equally well with several nonlinear functions based on the norm of least-square curve-fitting procedures (42). A modified logistic function was employed for curve fitting (26). Compared with other curve-fitting methods, one advantage of the logistic function used in this study is that the model parameters identified have clear physiological meanings (Fig. 1). In addition, the first-order derivative of the identified logistic function readily provides an estimation of CVMR for each level of P_{ETCO_2} .

The linear regression slope of the CBFV- P_{ETCO_2} relationship (CVMR0, 5%/Torr) over the entire range of changes in P_{ETCO_2} is consistent with previous findings (8, 14, 27, 40). However, this method of analysis, although practical, evidently underestimates the maximal cerebral vasodilatory effect of CO_2 , as indicated by the estimates of CVMRmax using either the first-order derivatives of the identified logistic function (8%/Torr) or the specific linear regressions in the steep portion of sigmoidal curves (7%/Torr) (Table 2).

The inflection point of the logistic function (parameter x_0), which corresponds to the maximal rate of changes in CBFV or CVCi to CO_2 (CVMRmax), was almost identical for both the CBFV- P_{ETCO_2} and CVCi- P_{ETCO_2} relationships (Table 2). This demonstrates that CVMRmax occurs during moderate hypercapnia, slightly above the baseline level of P_{ETCO_2} , consistent with previous studies suggesting that estimation of CVMR is lower during hypocapnia than during hypercapnia (13, 24, 40, 51).

Previous studies have used similar rebreathing methods to estimate CVMR (8, 20, 35, 51). However, these studies investigated only the hypercapnic stimuli and used linear regressions to derive a CVMR from 2.8 to 5.2%/Torr (8, 20, 35). Only one study included the hypocapnic range using hyperventilation before rebreathing and applied a bilinear model, resulting in a smaller CVMR in the hypocapnic range than in the hypercapnic range (1.6 vs. 2.8 $cm \cdot s^{-1} \cdot Torr^{-1}$) (51). Direct comparisons to these previous findings are difficult because hypoxic and/or hyperoxic conditions were also employed in these studies.

In conclusion, a clinically applicable rebreathing method was developed to assess CVMR during transient changes in P_{ETCO_2} . We found that both CBFV and CVCi responses to transient changes in P_{ETCO_2} are nonlinear and that these responses can be quantified well by a modified logistic function. Furthermore, we found that the magnitude of change in CBFV during CO_2 rebreathing (and hyperventilation) is higher than that of CVCi, suggesting direct effects of increases (and decreases) in ABP on changes in CBFV. For assessment of CVMR, the range of changes in CO_2 to be studied and the confounding influence of changes in ABP on CBFV must be considered for application of an appropriate modeling method to quantify CBFV or CVCi responses.

ACKNOWLEDGMENTS

We thank the subjects for participating in this study. We also thank Michael Ogawa for valuable assistance in this research.

GRANTS

This study was supported in part by a grant from The American Heart Association Texas Affiliate 0060024Y and a research scholarship to J. A. H. R. Claassen from the Radboud University Medical Center (Nijmegen, The Netherlands).

REFERENCES

1. Aaslid R, Lash SR, Bardy GH, Gild WH, Newell DW. Dynamic pressure-flow velocity relationships in the human cerebral circulation. *Stroke* 34: 1645–1649, 2003.
2. Ainslie PN, Ashmead JC, Ide K, Morgan BJ, Poulin MJ. Differential responses to CO_2 and sympathetic stimulation in the cerebral and femoral circulations in humans. *J Physiol* 566: 613–624, 2005.
3. Atkinson JL, Anderson RE, Sundt TM Jr. The effect of carbon dioxide on the diameter of brain capillaries. *Brain Res* 517: 333–340, 1990.
4. Bishop CC, Powell S, Rutt D, Browne NL. Transcranial Doppler measurement of middle cerebral artery blood flow velocity: a validation study. *Stroke* 17: 913–915, 1986.
5. Blaser T, Hofmann K, Buerger T, Effenberg O, Wallesch CW, Goertler M. Risk of stroke, transient ischemic attack, and vessel occlusion before endarterectomy in patients with symptomatic severe carotid stenosis. *Stroke* 33: 1057–1062, 2002.
6. Braune S, Hetzel A, Prasse A, Dohms K, Guschlbauer B, Lucking CH. Stimulation of sympathetic activity by carbon dioxide in patients with autonomic failure compared with normal subjects. *Clin Auton Res* 7: 327–332, 1997.
7. Busija DW, Heistad DD. Effects of activation of sympathetic nerves on cerebral blood flow during hypercapnia in cats and rabbits. *J Physiol* 347: 35–45, 1984.
8. Clivati A, Ciofetti M, Cavestri R, Longhini E. Cerebral vascular responsiveness in chronic hypercapnia. *Chest* 102: 135–138, 1992.
9. Dahl A, Lindegaard KF, Russell D, Nyberg-Hansen R, Rootwelt K, Sorteberg W, Nornes H. A comparison of transcranial Doppler and cerebral blood flow studies to assess cerebral vasoreactivity. *Stroke* 23: 15–19, 1992.
10. Duffin J, McAvoys GV. The peripheral-chemoreceptor threshold to carbon dioxide in man. *J Physiol* 406: 15–26, 1988.
11. Dumville J, Panerai RB, Lennard NS, Naylor AR, Evans DH. Can cerebrovascular reactivity be assessed without measuring blood pressure in patients with carotid artery disease? *Stroke* 29: 968–974, 1998.
12. Edvinsson L, Hamel E. Perivascular nerves in brain vessels. In: *Cerebral Blood Flow and Metabolism*, edited by Edvinsson L and Krause D. Philadelphia, PA: Lippincott Williams & Wilkins, 2002, p. 43–67.
13. Edwards MR, Topor ZL, Hughson RL. A new two-breath technique for extracting the cerebrovascular response to arterial carbon dioxide. *Am J Physiol Regul Integr Comp Physiol* 284: R853–R859, 2003.
14. Ellingsen I, Hauge A, Nicolaysen G, Thoresen M, Walloe L. Changes in human cerebral blood flow due to step changes in P_{aO_2} and P_{aCO_2} . *Acta Physiol Scand* 129: 157–163, 1987.
15. Giller CA, Bowman G, Dyer H, Mootz L, Krippner W. Cerebral arterial diameters during changes in blood pressure and carbon dioxide during craniotomy. *Neurosurgery* 32: 737–741, 1993.
16. Giller CA, Giller AM. A new method for fixation of probes for transcranial Doppler ultrasound. *J Neuroimaging* 7: 103–105, 1997.
17. Hancock SM, Mahajan RP, Athanassiou L. Noninvasive estimation of cerebral perfusion pressure and zero flow pressure in healthy volunteers: the effects of changes in end-tidal carbon dioxide. *Anesth Analg* 96: 847–851, 2003.
18. Harper AM, Glass HI. Effect of alterations in the arterial carbon dioxide tension on the blood flow through the cerebral cortex at normal and low arterial blood pressures. *J Neurol Neurosurg Psychiatry* 28: 449–452, 1965.
19. Harris J, Benedict F. A biometric study of human basal metabolism. *Proc Natl Acad Sci USA* 4: 370–373, 1918.
20. Hida W, Kikuchi Y, Okabe S, Miki H, Kurosawa H, Shirato K. CO_2 response for the brain stem artery blood flow velocity in man. *Respir Physiol* 104: 71–75, 1996.
21. Hopkins WG. Measures of reliability in sports medicine and science. *Sports Med* 30: 1–15, 2000.

22. Hsu HY, Chern CM, Kuo JS, Kuo TB, Chen YT, Hu HH. Correlations among critical closing pressure, pulsatility index and cerebrovascular resistance. *Ultrasound Med Biol* 30: 1329–1335, 2004.
23. Hurn P, Traystman RJ. Changes in arterial gas tension. In: *Cerebral Blood Flow and Metabolism*, edited by Edvinsson L and Krause D. Philadelphia, PA: Lippincott Williams & Wilkins, 2002, p. 384–394.
24. Ide K, Eliasziw M, Poulin MJ. The relationship between middle cerebral artery blood velocity and end-tidal PCO₂ in the hypocapnic-hypercapnic range in humans. *J Appl Physiol* 95: 129–137, 2003.
25. Jordan J, Shannon JR, Diedrich A, Black B, Costa F, Robertson D, Biaggioni I. Interaction of carbon dioxide and sympathetic nervous system activity in the regulation of cerebral perfusion in humans. *Hypertension* 36: 383–388, 2000.
26. Kent BB, Drane JW, Blumenstein B, Manning JW. A mathematical model to assess changes in the baroreceptor reflex. *Cardiology* 57: 295–310, 1972.
27. Kety S, Schmidt C. The effects of altered arterial tensions of carbon dioxide and oxygen on cerebral blood flow and cerebral oxygen consumption of normal young man. *J Clin Invest* 27: 484–492, 1948.
28. Kleiser B, Widder B. Course of carotid artery occlusions with impaired cerebrovascular reactivity. *Stroke* 23: 171–174, 1992.
29. Kontos HA, Richardson DW, Patterson JL Jr. Effects of hypercapnia on human forearm blood vessels. *Am J Physiol* 212: 1070–1080, 1967.
30. Lindegaard KF, Lundar T, Wiberg J, Sjöberg D, Aaslid R, Nornes H. Variations in middle cerebral artery blood flow investigated with noninvasive transcranial blood velocity measurements. *Stroke* 18: 1025–1030, 1987.
31. Mitsis GD, Ainslie PN, Poulin MJ, Robbins PA, Marmarelis VZ. Nonlinear modeling of the dynamic effects of arterial pressure and blood gas variations on cerebral blood flow in healthy humans. *Adv Exp Med Biol* 551: 259–265, 2004.
32. Mitsis GD, Zhang R, Levine BD, Marmarelis VZ. Cerebral hemodynamics during orthostatic stress assessed by nonlinear modeling. *J Appl Physiol* 101: 354–366, 2006.
33. Mohan R, Duffin J. The effect of hypoxia on the ventilatory response to carbon dioxide in man. *Respir Physiol* 108: 101–115, 1997.
34. O'Leary DS. Regional vascular resistance vs. conductance: which index for baroreflex responses? *Am J Physiol Heart Circ Physiol* 260: H632–H637, 1991.
35. Pandit JJ, Mohan RM, Paterson ND, Poulin MJ. Cerebral blood flow sensitivity to CO₂ measured with steady-state and Read's rebreathing methods. *Respir Physiol Neurobiol* 137: 1–10, 2003.
36. Panerai RB. The critical closing pressure of the cerebral circulation. *Med Eng Phys* 25: 621–632, 2003.
37. Panerai RB, Deverson ST, Mahony P, Hayes P, Evans DH. Effects of CO₂ on dynamic cerebral autoregulation measurement. *Physiol Meas* 20: 265–275, 1999.
38. Panerai RB, Evans DH, Naylor AR. Influence of arterial blood pressure on cerebrovascular reactivity. *Stroke* 30: 1293–1295, 1999.
39. Panerai RB, Simpson DM, Deverson ST, Mahony P, Hayes P, Evans DH. Multivariate dynamic analysis of cerebral blood flow regulation in humans. *IEEE Trans Biomed Eng* 47: 419–423, 2000.
40. Poulin MJ, Liang PJ, Robbins PA. Dynamics of the cerebral blood flow response to step changes in end-tidal PCO₂ and PO₂ in humans. *J Appl Physiol* 81: 1084–1095, 1996.
41. Poulin MJ, Liang PJ, Robbins PA. Fast and slow components of cerebral blood flow response to step decreases in end-tidal PCO₂ in humans. *J Appl Physiol* 85: 388–397, 1998.
42. Reivich M. Arterial PCO₂ and cerebral hemodynamics. *Am J Physiol* 206: 25–35, 1964.
43. Richardson DW, Wasserman AJ, Patterson JL Jr. General and regional circulatory responses to change in blood pH and carbon dioxide tension. *J Clin Invest* 40: 31–43, 1961.
44. Ringelstein EB, Sievers C, Ecker S, Schneider PA, Otis SM. Noninvasive assessment of CO₂-induced cerebral vasomotor response in normal individuals and patients with internal carotid artery occlusions. *Stroke* 19: 963–969, 1988.
45. Rohrbeg M, Brodhun R. Measurement of vasomotor reserve in the transcranial Doppler-CO₂ test using an ultrasound contrast agent (Levovist). *Stroke* 32: 1298–1303, 2001.
46. Serrador JM, Picot PA, Rutt BK, Shoemaker JK, Bondar RL. MRI measures of middle cerebral artery diameter in conscious humans during simulated orthostasis. *Stroke* 31: 1672–1678, 2000.
47. Shoemaker JK, Vovk A, Cunningham DA. Peripheral chemoreceptor contributions to sympathetic and cardiovascular responses during hypercapnia. *Can J Physiol Pharmacol* 80: 1136–1144, 2002.
48. Totaro R, Marini C, Baldassarre M, Carolei A. Cerebrovascular reactivity evaluated by transcranial Doppler: reproducibility of different methods. *Cerebrovasc Dis* 9: 142–145, 1999.
49. Valdeuz JM, Draganski B, Hoffmann O, Dirnagl U, Einhaupl KM. Analysis of CO₂ vasomotor reactivity and vessel diameter changes by simultaneous venous and arterial Doppler recordings. *Stroke* 30: 81–86, 1999.
50. Vallbo AB, Hagbarth KE, Torebjork HE, Wallin BG. Somatosensory, proprioceptive, and sympathetic activity in human peripheral nerves. *Physiol Rev* 59: 919–957, 1979.
51. Vovk A, Cunningham DA, Kowalchuk JM, Paterson DH, Duffin J. Cerebral blood flow responses to changes in oxygen and carbon dioxide in humans. *Can J Physiol Pharmacol* 80: 819–827, 2002.
52. Wei EP, Kontos HA, Patterson JL Jr. Dependence of pial arteriolar response to hypercapnia on vessel size. *Am J Physiol Heart Circ Physiol* 238: H697–H703, 1980.
53. Widder B, Kleiser B, Krapf H. Course of cerebrovascular reactivity in patients with carotid artery occlusions. *Stroke* 25: 1963–1967, 1994.
54. Wilson DA, Traystman RJ, Rapela CE. Transient analysis of the canine cerebrovascular response to carbon dioxide. *Circ Res* 56: 596–605, 1985.
55. Zhang R, Zuckerman JH, Iwasaki K, Wilson TE, Crandall CG, Levine BD. Autonomic neural control of dynamic cerebral autoregulation in humans. *Circulation* 106: 1814–1820, 2002.